



# **Analysis and Improvement of Traction Motor Insulation Systems Exposed to High Switching Frequency Converters**

Master Thesis in Electrical Power Engineering

Mohammed Numair Alhalak



MASTER'S THESIS IN ELECTRICAL POWER ENGINEERING 2021

**Analysis and Improvement of Traction Motor  
Insulation Systems Exposed to High Switching  
Frequency Converters**

Mohammed Numair Alhallak



**CHALMERS**  
UNIVERSITY OF TECHNOLOGY

Department of Electrical Power Engineering  
CHALMERS UNIVERSITY OF TECHNOLOGY  
Gothenburg, Sweden 2021

Analysis and Improvement of Traction Motor Insulation Systems Exposed to High Switching Frequency Converters

Mohammed Numair Alhallak

©Mohammed Numair Alhallak, 2020

Supervisors:

Dr. Xiaoliang Huang, Chalmers University of Technology

Dr. Shafiqh Nategh, ABB Traction Motor

Examiner:

Professor Yujing Liu, Chalmers University of Technology

Department of Electrical Power Engineering

Chalmers University of Technology

SE-412 96 Gothenburg

Sweden

Telephone: +46(0)31-772 1000

Analysis and Improvement of Traction Machine Insulation Systems Exposed to High Switching Frequency Converters  
Mohammed Numair Alhallak  
Department of Electrical Power Engineering  
Chalmers University of Technology

## Abstract

High switching frequencies are used in converters of electric machines to improve their efficiencies. However, the high switching frequencies result in high voltage difference between conductors, which has a significant effect on insulation lifetimes of electric machines [1]. In this thesis work, insulation lifetime tests of winding samples are performed under repetitive impulse voltage. The impacts of insulation material types and environmental conditions on winding lifetimes are studied.

An electrical circuit is built up to generate a high impulsive voltage at two different levels (3kV and 3.5kV). This impulse voltage is applied to winding samples with taped insulation material. The charge and discharge occur as long as the applied voltage is higher than the partial discharge inception voltage (PDIV) during the tests. In addition, The insulation tests has been implemented at two different levels of temperature (150 and 180 degrees). The results indicate that due to the different levels of voltage and temperature, winding samples can have different insulation lifetimes. The lifetimes of winding insulation becomes shorter with higher voltage and temperature. It is also observed that corona resistance materials increase the lifetime compared with non-corona resistance materials.

Keywords: Electric machine lifetime, high-frequency converter, stator winding insulation; corona resistance.

# Acknowledgements

This work has been done within Chalmers university of technology and ABB company. I am grateful to my examiner, Prof. Yujing Liu for giving me the support, promoting, providing ideas and questions that keep me alert.

My supervisor in industry, Dr. Shafigh Nategh whom I had an opportunity to benefit from. He helped me to communicate with other companies that were useful for my project. He was always ready to discuss the different issues that were related to my project. Furthermore, He had been ready for sharing his valuable ideas that were very helpful.

My supervisor in Chalmers, Dr Xiaoliang Huang had helped me in the Laboratory experiment and the theory part. Moreover, we had discussed many interesting things that were useful for understanding the project overall.

Also I will thank Mr. Bowen Jiang, the doctoral candidate in EPE department for his help all the time.

I would thank Shawn Filliben, Edith Serafini and Olga Buldakova from Dupont for supplying the materials and also their technical support throughout this project. Also, I thank Dahrentråd AB for their support in production of samples.

Last but not least, my parents are thanked for all supports, they always encourage me to keep on and fight in order to achieve my goal in this life. They are the ones who help me to be the person I am today.

Mohammed Numair Alhallak  
Gothenburg, Sweden  
November 2020

---

## Publications

- [1] X. Huang, B. Jiang, M. N. Alhallak, S. Nategh, Y. Liu and A. Boglietti, "Experimental Evaluation of Conductor Insulations Used in E-mobility Traction Motors," 2021 IEEE Workshop on Electrical Machines Design, Control and Diagnosis (WEMDCD), 2021, pp. 249-253, doi: 10.1109/WEMDCD51469.2021.9425683.
- [2] M. N. Alhallak, S. Nategh, X. Huang, B. Jiang,, Y. Liu and A. Boglietti, "Experimental Evaluation of Conductor Insulations Used in E-mobility Traction Motors," IEEE Transactions on Industry Applications, Submitted.

# Contents

<b>1</b>	<b>Introduction</b>	<b>1</b>
1.1	Aim . . . . .	2
<b>2</b>	<b>Literature Study</b>	<b>3</b>
2.1	Electric Machines and Applications in E-mobility . . . . .	3
2.1.1	Types of Electric Machines . . . . .	3
2.1.1.1	DC Brush Machines . . . . .	3
2.1.1.2	Brushless DC Machines (BLDC) . . . . .	4
2.1.1.3	Permanent Magnet Synchronous Machines (PMSM) . . . . .	4
2.1.1.4	Induction Machines . . . . .	4
2.1.1.5	Switched Reluctance Machines (SRM) . . . . .	5
2.1.2	The Most Popular Machines in E-mobility . . . . .	6
2.2	Winding Insulation Failure Mechanism . . . . .	7
2.3	Traction Machine Insulation Systems . . . . .	8
2.4	Voltage Difference in Hairpin Winding Exposed to High Switching Frequencies . . . . .	8
2.5	Hairpin Winding Configurations . . . . .	10
2.5.1	Winding Configuration I . . . . .	10
2.5.2	Winding Configuration II . . . . .	11
2.5.3	Effects of Winding Layout on Voltage Distribution . . . . .	11
2.6	High-Frequency Equivalent Circuit Modeling Methods . . . . .	12
2.7	The Effect of Impulse Voltage Parameters on PD Feature . . . . .	13
2.8	Insulation Lifetime . . . . .	14
<b>3</b>	<b>Methods</b>	<b>17</b>
3.1	Electrical Circuit . . . . .	17
3.1.1	Electrical Circuit with Current Sensors . . . . .	17
3.1.2	Electrical Circuit with Voltage Sensors . . . . .	18
3.2	The Test Procedures . . . . .	20
<b>4</b>	<b>Experiment Design</b>	<b>21</b>
4.1	Winding Insulation Samples . . . . .	21
4.1.1	Kapton® FN . . . . .	21
4.1.2	Kapton® FCR . . . . .	21
4.1.3	Kapton® FCRC . . . . .	21
4.1.4	Kapton® EWS . . . . .	21

4.1.5	Kapton® ECRC . . . . .	21
4.1.6	Kapton® PRN . . . . .	21
4.2	Experimental Set-ups . . . . .	22
4.3	Experimental Control Strategies . . . . .	25
<b>5</b>	<b>Results</b>	<b>28</b>
5.1	Simulation Results . . . . .	28
5.2	Experimental Results . . . . .	30
5.2.1	FN At 180 Degrees And 3.5 Kv . . . . .	30
5.2.2	ECRC67 At 180 Degrees And 3.5 kV . . . . .	30
5.2.3	ECRC53 At 180 Degrees And 3.5 Kv . . . . .	31
5.2.4	ECRC53 At 150 Degrees And 3.5 Kv . . . . .	31
<b>6</b>	<b>Discussion</b>	<b>33</b>
<b>7</b>	<b>Conclusions</b>	<b>36</b>
	<b>Bibliography</b>	<b>37</b>

# 1

## Introduction

Due to needs of transforming to a low-carbon society as well as obtaining zero-emission transportation, many researchers and innovators are working on improving traction machine operations in the e-mobility market. The improvement and enhancement of the traction machine operation are important in order to employ the traction machine in the e-mobility market. Traction machines have been used in railway transportation for many years. They have been designed to deal with harsh environments. However, efficiency of the traction machines in railway applications was not prioritised [3]. Recently, many companies such as ABB have started to use their traction machines in the e-mobility market. The first application is electric buses. The transformation from the railway applications to the e-mobility market has faced many difficulties such as performance requirements and configurations of propulsion systems.

High switching frequencies are applied to converters of traction machines to improve their performance and efficiencies. This can be achieved by replacing the silicon (SI) semiconductor to the converter with silicon carbide (SIC) semiconductor [2]. This provides high switching frequencies, lower losses and less needs of cooling. Harmonic losses, which are generated due to connection with the converter, are reduced by increasing the switching frequency [1,4]. However, higher switching frequency means higher electrical stress on insulation systems of electric machines. The high electrical stress is usually solved by increasing the thickness of insulation material [1]. However, this increase will reduce electric machine efficiencies. This is because that increase in insulation system leads to an increase in the fundamental losses. Therefore, the existing insulation systems, which are exposed to fast switching and rising voltage, should be understood and investigated to be able to handle the high electrical stress.

Partial discharge (PD) provides valuable information in order to develop insulation materials. The dielectric of insulation material is built upon additional currents that occur during and after PD activities. These additional currents could be reduced by increasing the insulation resistance of the material. The higher the resistance of insulation material, the better the handling of electrical stress. For example, ECRC67 has higher resistance than ECRC53. This is because ECRC67 has more number of layers (higher overlap percentages). Therefore, it is more reliable to handle voltage stresses generated from the fast switching-frequency converters. As a result, the operation of the traction machine will be more reliable than before. One solution to improve the performance of the insulation system could be achieved by using corona resistance insulation materials to handle the high voltage stress. In order to induce high electrical stress, winding samples of taped with insulation polymer material

are exposed to high impulse voltage. The applied voltage is higher than the partial discharge inception voltage (PDIV) at two different levels (3kV and 3.5kV). These samples are put in the oven with two levels of temperature (150 and 180 degrees). It is important to determine the lifetimes of the winding sample insulation. Therefore, they are exposed to high frequency (high electrical stress) to accelerate their aging. In this study, the lifetimes of these samples will be investigated for different levels of temperature and voltage.

### **1.1 Aim**

The aim of this project is to improve the efficiency and reliability of the traction machine which is fed by converter. The limitation of the insulation system which is exposed to high electrical stress should be known. In addition, the factors which affect the insulation system such as temperature, voltage level and insulation tape overlap percentage, should be studied.

# 2

## Literature Study

### 2.1 Electric Machines and Applications in E-mobility

Electric machines are used in many electric devices such as electric cars, drones. They are used to convert electrical energy to mechanical energy and vice versa. There are two categories of electric machines based on power supply either DC machines or AC machines [21].

#### 2.1.1 Types of Electric Machines

Electric machines are not new technologies but there is a huge interest in using them in electric vehicles because they are needed to reduce the pollution in this world. The Internal Combustion engines are replaced by electric machines. Electrical machines are connected with electric batteries and power electronics that are improved frequently [19]. There are some electric machines that are described as follow.

##### 2.1.1.1 DC Brush Machines

This type is suitable for traction applications such as railway. It is characterised by high starting torque and ease of speed control. In addition, It has the capability to face the sudden increase in load. This type needs frequent maintenance that is considered as a drawback due to the brushes [19]. The structure of DC brush machines is shown in Figure 2.1 as follow.

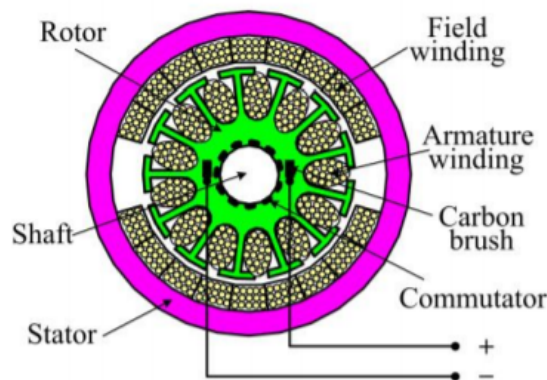
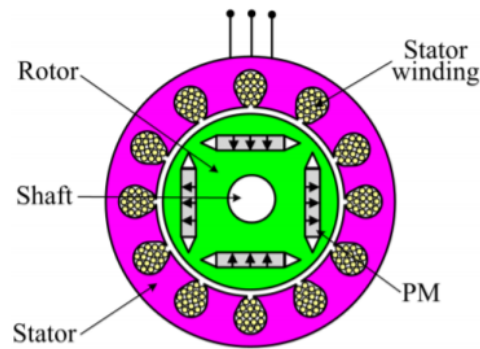


Figure 2.1: DC brush machine [20]

### 2.1.1.2 Brushless DC Machines (BLDC)

The advantage of this type of machine compared with the previous one is less maintenance because of the brushless. The brushes are done electronically. Brushless DC machine (BLDC) is most used in the electric vehicle due to its characterised such as high starting torque and high efficiency around 98 percents [19]. The structure of DC brushless machines is shown in Figure 2.3 as follow.



**Figure 2.2:** Brushless DC machine [20]

### 2.1.1.3 Permanent Magnet Synchronous Machines (PMSM)

Permanent Magnet Synchronous machine is similar to brushless DC machine. The only difference is that back electromagnetic field (EMF) is trapezoidal for (BLDC) whereas it is sinusoidal for (PMSM). PMSM is competitive to other electric machines despite of its high cost. It is used in applications that demand high performance and efficiency such as cars, trucks and buses. It is also characterised with high power rating [19].

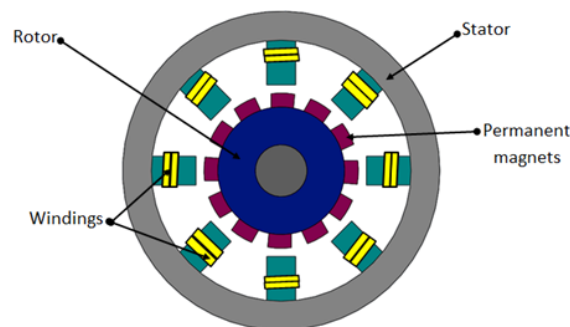


**Figure 2.3:** Permanent Magnet Synchronous Machines [23]

### 2.1.1.4 Induction Machines

Induction machines do not have high starting torque under constant voltage or frequency compared with the high starting torque in PMSM. However, this characteristic can be improved through the voltage/frequency method. It can provide

high starting torque by the  $v/f$  method. Then, an induction machines can be used in traction applications. This method can be used to control or adjust the flux density depending on torque requirements as illustrated in Figure 2.4. The drawback of the induction machine is its complex control system [19].

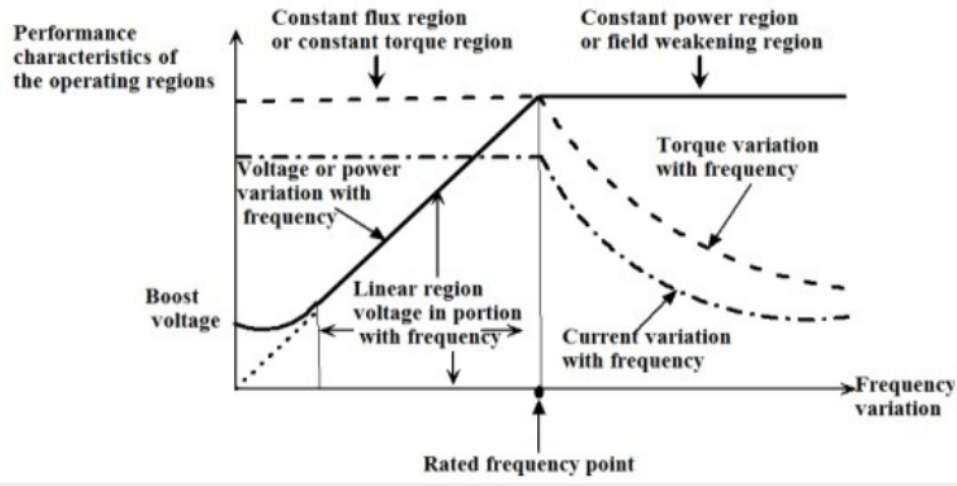


**Figure 2.4:** Induction machine performance characteristics [20]

The structure of induction machines is shown in Figure 2.5 as follow.

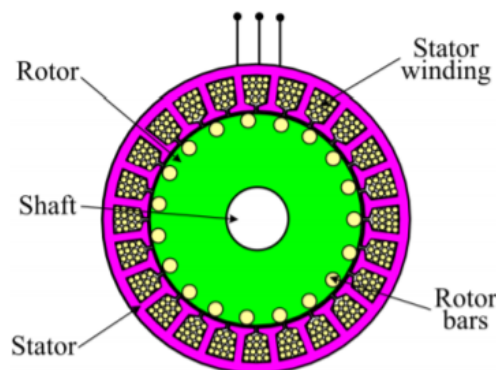


**Figure 2.5:** Induction machine [20]

### 2.1.1.5 Switched Reluctance Machines (SRM)

The structure of switched reluctance machines is simple. The rotor consists of steel laminated instead of permanent magnets. This makes the inertia is less and it can accelerate quickly. As a result, this machine is suitable for high-speed applications. In addition, the heat is only concentrated in the stator due to the windings. Thus, the cooling system is simple. The drawback of this machine is that the control system is complex [19]. The structure of SRM is shown in Figure 2.6 as follow.

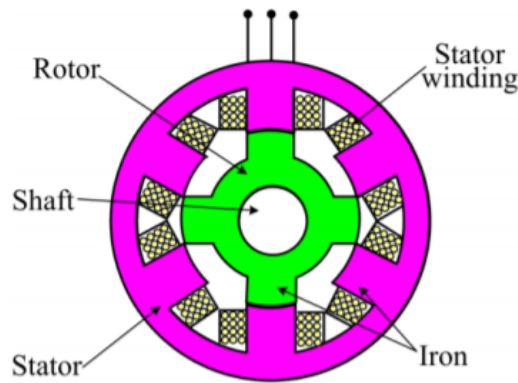


**Figure 2.6:** Switched Reluctance machine [20]

### 2.1.2 The Most Popular Machines in E-mobility

PMSM has many advantages that are appropriated to EV and HEV. It is used in applications that demand high starting torque, high speed and high power range. Therefore, it is used in applications like cars, trucks and buses. However, the cost and the limited materials are considered as drawback. Therefore, SRM is a good choice for EV and HEV due to their low cost and strong structure [23]. In addition, other benefits that makes SRM are competitive to other electric machines. Nowadays EV and HEV are using PMSM, induction machine and BLDC. The new technology has introduced a rare-earth-free machines such SRM. They have a simple structure where there is no windings and permanent magnets on the rotor. The most important factors that make EV and HEV effective are cost, weight and efficiency. All these factors could be achieved by using SRM. The advantages behind using SRM in EV and HEV are high power density, high starting torque, high efficiency and good performance [24]. According to the table below, SRM is a good choice in EV and HEV application. Higher number of digit is good for the choice in e-mobility applications.

Items	Maximum	BLDC	PMSM	SRM
Power density	10	9	10	8
Overload	10	7	7	8
High speed range	20	9	10	8
Control	20	15	15	16
Noise	10	8	8	6
Torque ripple	10	6	8	5
Size and weight	10	8	9	7
Ruggedness	20	14	12	18
Maintenance	10	8	8	9
Manufacturing	20	14	12	18
Cost	30	20	18	26
Total	180	128	135	146

**Table 2.1:** Comparison between the electric machines [24]

## 2.2 Winding Insulation Failure Mechanism

The traction machine is connected with inverter. The pulse width modulation technology is utilized to generate sinusoidal voltage source. This can be done by using MOSFET. The fast rise time voltage wave travels to the machine terminal and the reflection will occur due to the difference in impedance between the cable and the traction machine. The reflection wave travels back to the inverter and induces other reflection due to the difference in impedance between the cable and the inverter [16]. This reflection will overlap the square wave voltage and induce overshoot at the front of voltage wave as seen in Figure 2.7.

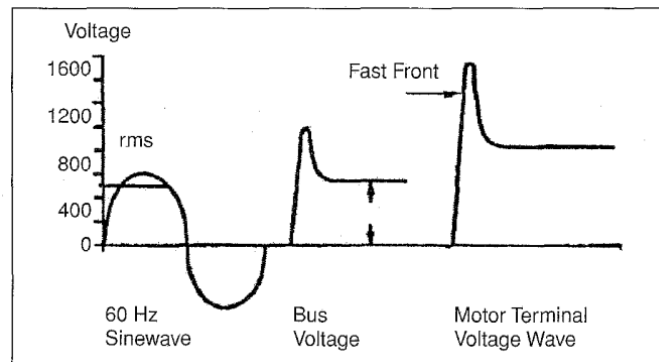


**Figure 2.7:** The voltage stress due to the reflection [16]

The resulting overshoot depends on the length of the cable and the voltage rise time. Therefore, if the cable is longer, the overshoot is higher. As result, the output voltage on the machine terminal has spikes. These spikes magnitude depends on combined factors as follow

- The voltage rise time.
- The length of the cable.
- The high frequency.

These factors cause the early failure of the insulation machine. It is important to understand the failure mechanism in order to design the insulation system of the electric machine. It is observed that charges accumulates at the insulation surface that is exposed to an impulse voltage with fast rise and fall edges. The occurrence of the insulation failure depends on different effects such as partial discharge, dielectric heating and the initial electron charge. Understanding the mechanism of the failure is useful in order to an increase the lifetime of the insulation. Increasing the lifetime of the insulation is possible as follow

- Decrease the length of the cable that connects the inverter and the machine to get a lower overshoots or spikes.
- Reduce the harmonics by increasing the fall and rise pulse width modulation through adding a low pass filter.
- Add more insulation at the end of the turn and the slots.

## 2.3 Traction Machine Insulation Systems

Due to the expansion in using the electric machines and power electronic, the electrical insulation components should be improved in order to cope with the high electrical stress. The insulation materials should have a good performance regarding the reliability of electrical machines. The insulation materials are used in different applications due to the properties that are available for different demanding engineering application such as the handling of electrical stress or high temperature. The challenge with the improvement in the electrical insulation materials is obtaining a free or minimum partial discharge. The partial discharge inception voltage (PDIV) will increase with added material to insulation. The benefit of the added material is an increase in the insulation lifetime under the high-electrical stress. If the thickness of the regular insulation and the added insulation material is the same then the efficiency and the reliability of the traction machine is high [18].

## 2.4 Voltage Difference in Hairpin Winding Exposed to High Switching Frequencies

Hairpin winding is used in EV machine in order to satisfy the high demands on the torque and power density. The conductors of this type of winding have a rectangular cross area section. These conductors are inserted in the stator slots. Their endings are twisted and welded to the following conductor to form wave windings. The phase conductors are connected in series or parallel. The connection is called Special Connections (SCs) [12]. There are some benefits of using hairpin windings. These benefits are that the cost and production-time are reduced because the SCs are limited. Moreover, the circulating currents are eliminated when parallel paths are required through a proper winding transposition [15].

An increase in the switching frequency leads to an increase in electrical stresses due to the high  $dv/dt$ . In order to minimize the electrical stress, the size of the insulation system could be increased. However, the fundamental losses will be higher at bigger size of insulation system. This increase of fundamental losses causes a lower efficiency and energy of traction machine [1,5,8,9]. The rising time of the input voltage in the range (30-600) ns is considered as a high electrical stress. The amplitude of the input voltage is fixed at VDC= 1000 V, with a slew rate  $dv/dt$  in the range 33–2 kV/s as shown in Figure 2.8.

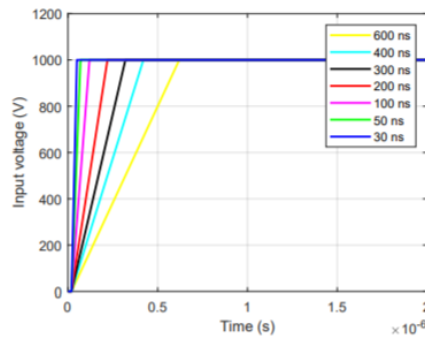


**Figure 2.8:** A-phase voltage inputs [12]

The voltage difference between conductor 1 and conductor 2 increases at lower rise time voltage and vice versa. As seen in Figure 2.9 all the waveforms are compared with the one that its rise time is 300 ns [12].

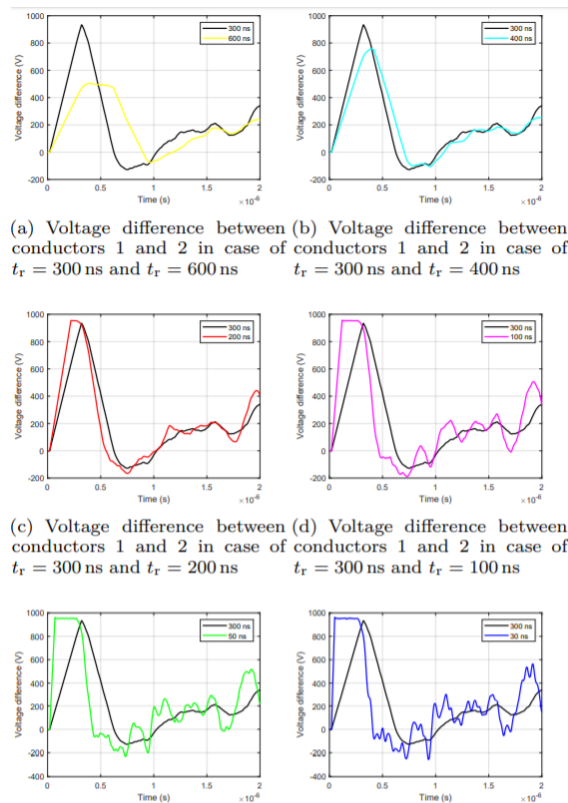


**Figure 2.9:** Voltage differences between conductor one and two [12]

The conductor insulation should be designed at the voltage level where its rising time is lower than 300 ns. As seen in Figure 2.10 the characteristic of the voltage versus rise time. It is noted that the voltage differences between conductor 1 and conductor 2 are full voltage for a rising time lower than 300 ns [12].

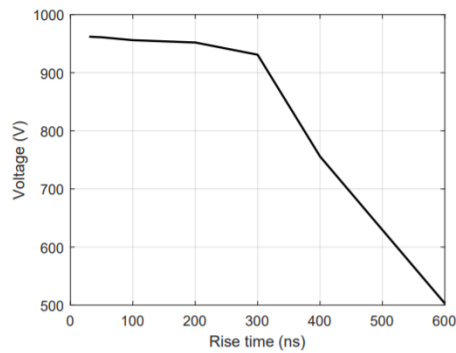


**Figure 2.10:** Voltage versus rise time of the actual machine winging [12]

## 2.5 Hairpin Winding Configurations

There are two different types of winding configurations as follow.

### 2.5.1 Winding Configuration I

The First Winding Configuration (FWC) is illustrated in Figure 2.11 [12]. Let consider Figure 2.11. As seen the first rotation is presented by the black path. The black path occupies the first and second layer. After a full rotation the first and second path connect each other with special connection that is called  $L2 \rightarrow L2$ . This special connection is characterized by the same pitch but different shape because it connects two sides in the same layer. The second path, which is reported in gray color, occupies the second and first layer in counter clockwise direction in order to provide a free space for other phases. The ending point of this path is located in the first layer  $L1$  and connected to the third path (blue color Figure 2.11 that is located in the third layer). This special connection allows to jump between first and third layers  $L1 \rightarrow L3$ . The last connection is between third and fourth paths. This connection is called  $(L4 \rightarrow L4)$  that has the same shape of  $L2 \rightarrow L2$  but different layer.

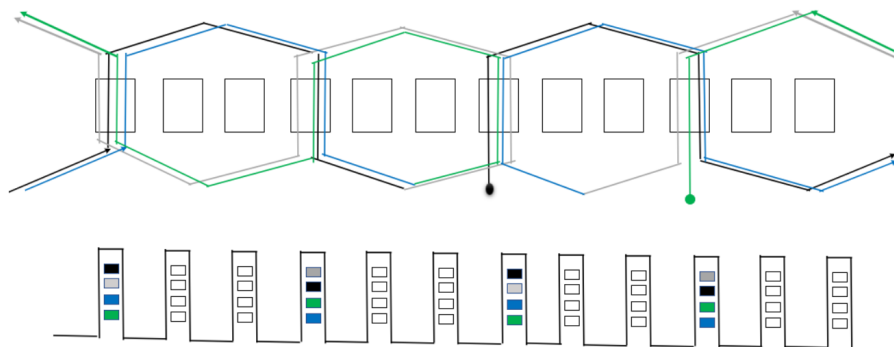


**Figure 2.11:** Phase-A winding configuration I

### 2.5.2 Winding Configuration II

Another connection for A-phase is called Second Winding Configuration (SWC) [12]. This connection scheme is illustrated in Figure 2.12. This connection is characterised by the second path (gray color) occupies the third and fourth layers and moves clockwise. Thus, The first special connections (SCs) is between the second to the third layer  $L2 \rightarrow L3$ . The second special connection is between the same layer (the fourth layer)  $L4 \rightarrow L4$ . The last connection is between the third and second layer  $L3 \rightarrow L2$ .

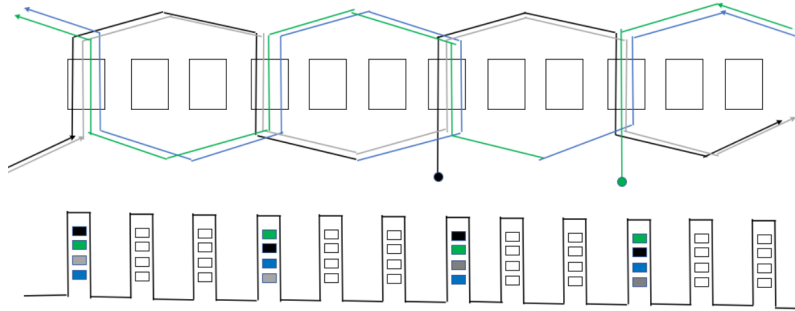


**Figure 2.12:** Phase-A winding configuration II

This connection SWC is characterized by the maximum jump is one layer whereas FWC is characterized by two layers jump. Thus, the manufacturing process for FWC is more complicated than SWC due to the length of the jump.

### 2.5.3 Effects of Winding Layout on Voltage Distribution

The winding layout has influence on the voltage distribution in the actual machine winding. It is noticed that the voltage difference between conductor 1 and conductor 2 is lower for SWC compare with FWC. This is because that the length of the path which, connects conductor 1 and 2 in SWC, is longer than the path in FWC. As illustrated in Figure 2.13 the voltage difference with a rise time lower than 200 ns is almost full voltage difference in case of FWC, while the voltage difference for the same input voltage is lower in case SWC [12].

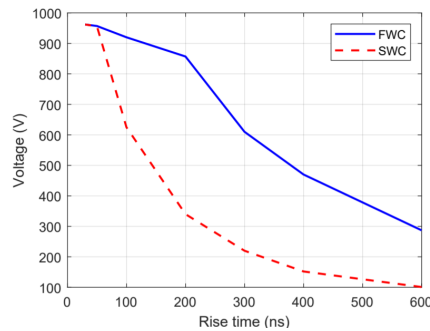


**Figure 2.13:** Voltage versus rise time with different special connections [12]

## 2.6 High-Frequency Equivalent Circuit Modeling Methods

In order to calculate the inter-turn voltage, a high-frequency machine winding equivalent circuit model is developed as following [12]. Lets consider first turn that is illustrated in Figure 2.14. Each turn is modeled through a zeta-section and it is characterized by end-winding and active parts. As seen in Figure 2.14 the turn occupies the first and second layer.



**Figure 2.14:** The first turn has active sides in first and second layers [12]

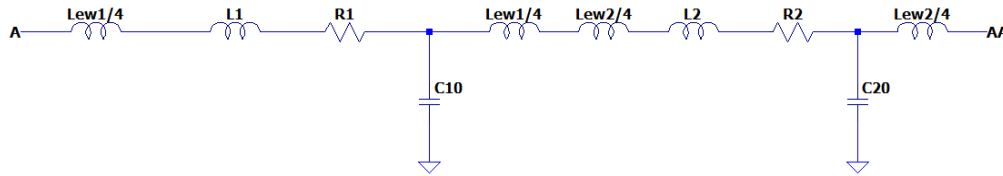


**Figure 2.15:** First turn equivalent circuit

The first turn, which is illustrated in Figure 2.14, is represented by equivalent circuit in Figure 2.15 where half turn is modeled with a  $\gamma$ -section and has the first slot parameters that are: slot and end winding inductances  $L_i$  and  $L_{ewi}$ , slot resistance  $R_i$  and line to ground capacitance  $C_{i0}$ , where  $i$  refers to the corresponding layer. The other half turn is modeled  $\gamma$ -section with the same parameters but relate to the second layer. As seen in Figure 2.15 the mutual capacitances between conductors are not considered. In order to model the first conductor that is moving between the first and second layer with  $q=2$  and the number of poles  $p=10$ , ten equivalent sub-circuit should be series connected, as illustrated in Figure 2.16. The other three conductors are modeled in the same way as first one.

To properly model the mutual capacitance between neighbor conductors should be included in the two slot equivalent circuit where is illustrated in Figure 2.17. Here the model is simplified where the mutual capacitance is added and both end winding and active inductances is considered through a single inductance  $L_i$  [12].

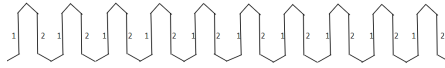


**Figure 2.16:** First conductor schematic representation [12]

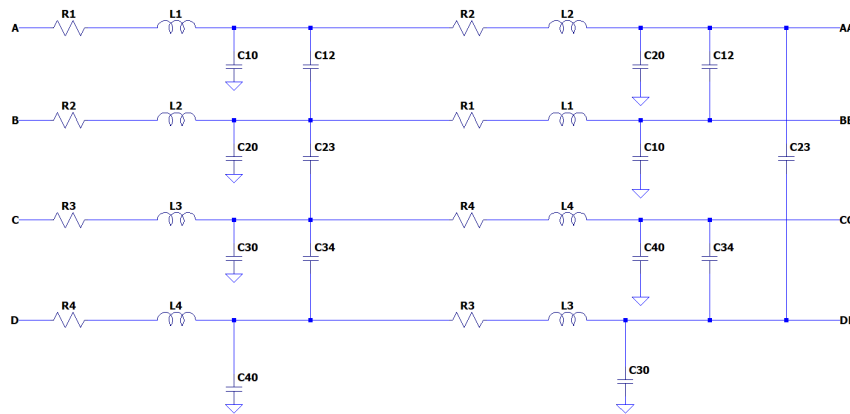


**Figure 2.17:** Two-slot equivalent circuit with inter-turn capacitances [12]

## 2.7 The Effect of Impulse Voltage Parameters on PD Feature

In order to select and improve the insulation materials, the study of partial discharge (PD) activity is important. This is because that dielectric materials are affected by partial discharge. PD indicates to dielectric response. It is considered as an excess currents occurs inside the dielectric as long as the voltage level is higher than (PDIV) [13,15]. The dielectric of machine winding could be decayed due to the partial discharge activities.

The power electronics, which is connected to the machine, affects the insulation reliability. This is because that pulse wave voltage with high frequency will be distributed unequally on the turns in the stator winding insulation. To improve the reliability of the insulation system, the endurance test is executed to determine the lifetime of the insulation for specific voltage and frequency. The insulation lifetime test can be performed by exposing the insulation to a square wave voltage. It is interested to study the effect of square wave voltage parameters on PD features. These parameters are voltage rise time, frequency and duty cycle. It is observed that the voltage rise time has a big influence regarding an accelerate the ageing of the insulation system. This is because the voltage rise time has an effect to cause PD that is considered the reason behind accelerating the ageing. The shorter rise time of square wave voltage induces lower lifetime of the insulation due to the higher partial discharge [17]. The another factor is the impulse voltage frequency. The higher frequency of square wave voltage lower PD magnitude [17]. As seen in Figure 2.18 there are different values of frequency 2 Hz, 20 Hz, 200 Hz, 2000 Hz as function of

PD magnitude.

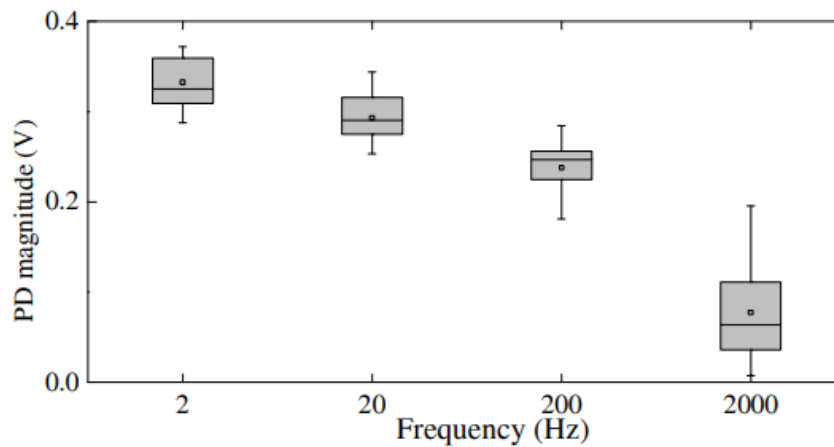


**Figure 2.18:** The effect of impulse voltage frequency on PD magnitude [17]

The third factor is the duty cycle of the impulse voltage. Longer duty cycle higher partial discharge magnitude until a specific value of duty cycle then it will be constant partial discharge value. There are no partial discharge events for very low duty cycle. There are different values of duty cycles as function with PD magnitude as illustrated in Figure 2.19

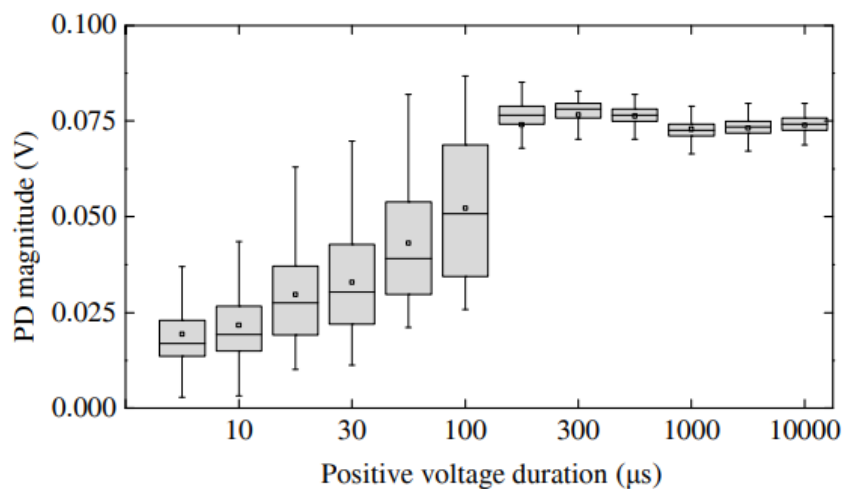


**Figure 2.19:** The effect of duty cycle duration on PD magnitude [17]

## 2.8 Insulation Lifetime

The lifetime test is done by applying impulse voltage to the insulation system. However, the rise time is hard to control and it is easy to change by changing the circuit parameters such as object test (capacitance), resistance and inductance. Therefore, the effect of rise time of the impulsive voltage on the final lifetime test is significant [14]. It is found that rise time of the impulsive voltage has an effect on PD features.

As seen in Figure 2.20 the lifetime test of the insulation as function of sinusoidal and impulse voltage. It is observed that the average lifetime decrease with decreasing the rise time of the impulse voltage. At voltage frequency 1 KHz, the lifetime with 50ns impulse voltage rise time is 1.5 times shorter than obtained when the impulse voltage rise time is 1us. Therefore, the impulse voltage rise time has a significant

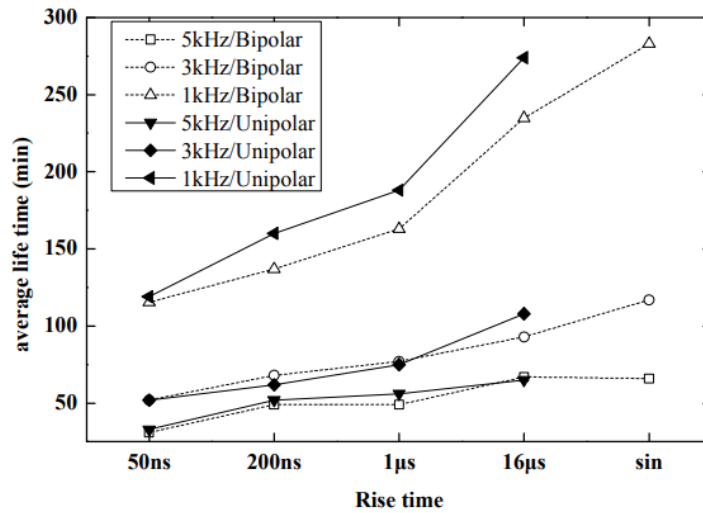


**Figure 2.20:** The effect of impulse voltage rise time as function with the insulation lifetime [14]

effect on the average lifetime of the insulation compare with the sinusoidal waveform. As illustrated in Figure 2.21 the failure time is much shorter when the insulation is exposed to shorter rise time of impulse voltage compare with the sinusoidal voltage.

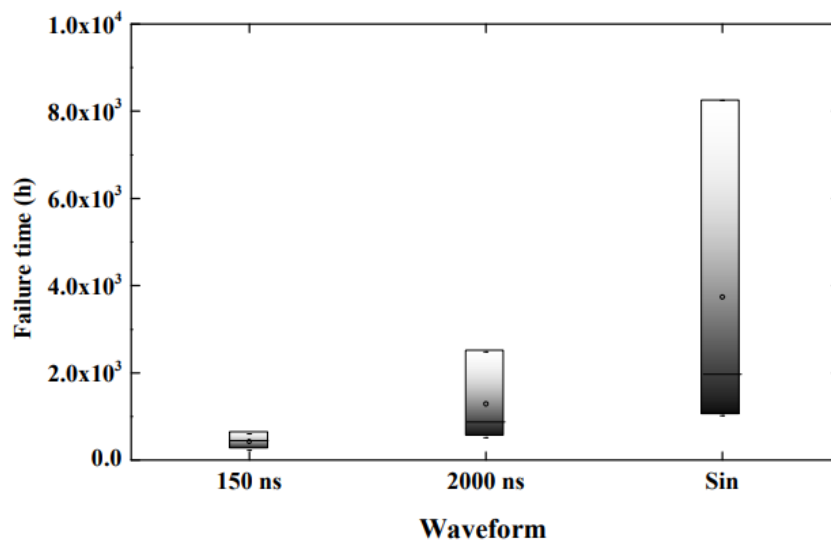


**Figure 2.21:** Failure time as function with impulse voltage rise time and sinusoidal voltage waveform [14]

To understand the reason behind the decay of the insulation lifetime with the shorter

impulse voltage rise time. The partial discharge magnitude increases with the shorter voltage rise time. Increasing PD magnitude is the reason behind the decay of the insulation lifetime. As shown in Figure 2.22 the PD magnitude decrease as rise time increases.

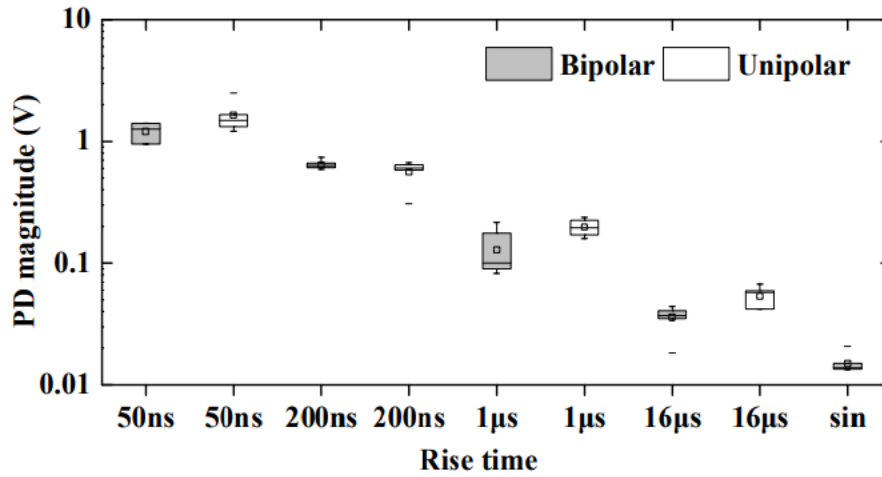


Figure 2.22: PD magnitude as function voltage rise time [14]

# 3

## Methods

### 3.1 Electrical Circuit

The electrical circuit is built to accelerate ageing experimental. In order to test and evaluate the winding insulation samples, high repetitive impulse voltage is applied. In fact, there are two types of the electrical circuit according to the sensor that is placed. The first one is designed with current sensors and the second one is designed with voltage sensors. Both circuits have the same function but the difference is the type of sensors. They are both described in detail as follow

#### 3.1.1 Electrical Circuit with Current Sensors

The electrical circuit is designed to be as shown in Figure 3.1

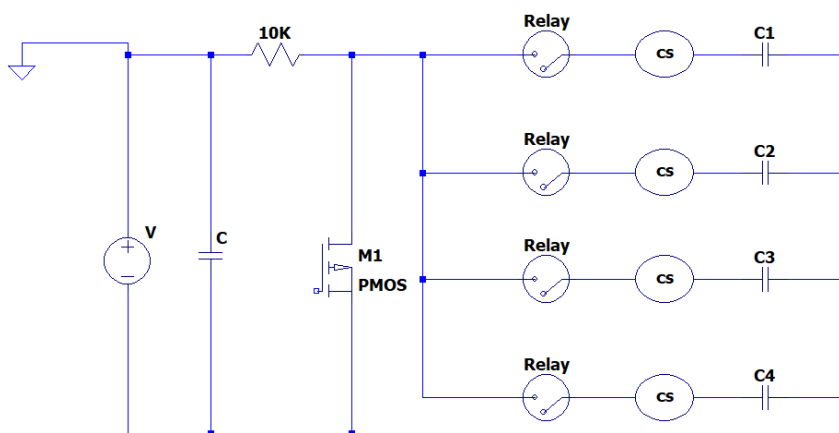


**Figure 3.1:** Electrical circuit schematic (current sensors)

High voltage power supply (V) is connected in parallel with a capacitor (C) in order to stabilize the voltage. The resistance 10 Kohm is placed for safety purpose. Four insulation samples are represented by four capacitors(C1-C4). They are connected in parallel in four branches. Each branch has one capacitor that is connected with the current sensor (cs) and relay. To generate a square wave voltage across the insulation samples, the switch (M1) is controlled to be on and off. The switches of four relays are kept on at the beginning. The capacitors that represent the winding samples (C1-C4) are charged by the source voltage when the switch (M1) is off. The capacitors (C1-C4) are discharged when the switch (M1) is on.

The issue is that there is overshoot in the current when the capacitance is discharging during a very short time as illustrated in Figure 3.2 . This overshoot flows in the current sensors that in turn send a wrong signals to the relays to open their switch.



**Figure 3.2:** The overshoot of the current due to the winding sample

As a result, there is no possibility to use the current sensors in this test in order to evaluate the winding insulation lifetime. The best solution is to use voltage sensors instead of current sensors.

### 3.1.2 Electrical Circuit with Voltage Sensors

High voltage power supply (V) is connected in parallel with capacitor (C) in order to stabilize the voltage. Four insulation samples are represented by four capacitors (C1-C4). They are connected in parallel in four branch. Each branch has one capacitor is connected with two resistors (10,1) Kohm, one relay and one filter. To generate a square wave voltage across the insulation samples, the switch (M1) is controlled to be on and off. The switch of four relays are kept on at the beginning. The capacitors that are represent the winding samples (C1-C4) are charged by the source voltage when the switch (M1) is off. The capacitors (C1-C4) are discharged in two resistors 10 Kohm and 1 Kohm when the switch (M1) is on. The electrical circuit is shown in Figure 3.3

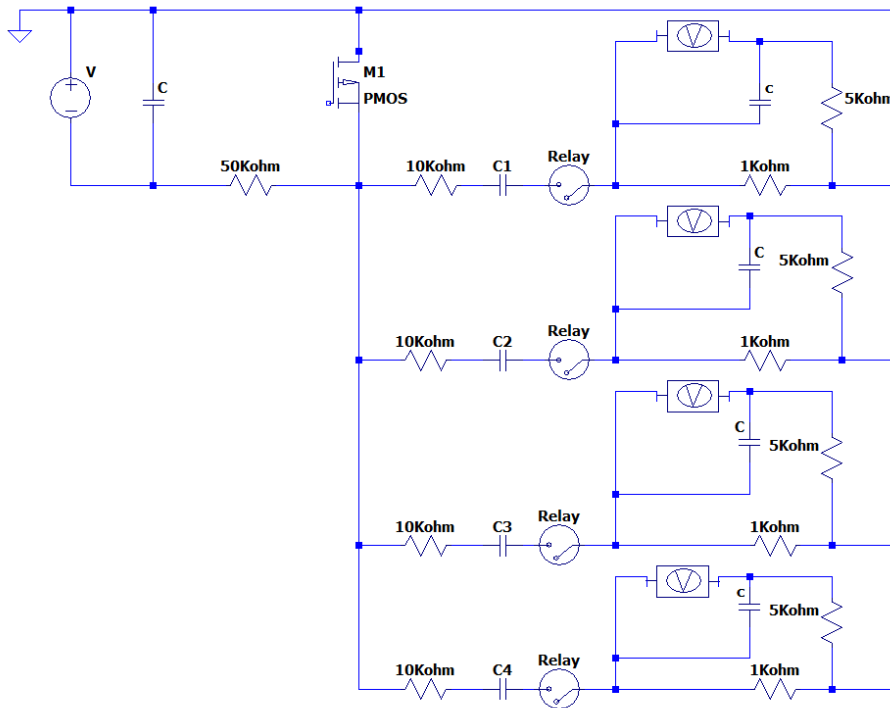


**Figure 3.3:** Electrical circuit schematic (voltage sensors)

The applied voltage across the insulation samples can be as derivatives but it can be as square wave voltage. The equation of applied voltage across winding samples is expressed as follow [22]

$$V_{sample} = V * (1 - e^{-t/T}) \quad (3.1)$$

For  $0 \leq t < t_0 * (1-D)$

$$V_{sample} = V * e^{-t/T} \quad (3.2)$$

For  $t_0 * (1-D) \leq t < t_0$

Where  $V_{sample}$  is the voltage across the insulation winding sample,  $V$  is the source voltage,  $t_0$  and  $D$  are cycle period and duty cycle,  $T$  is the time constant. 1 Kohm resistor is connected in parallel with the voltage sensor and (RC) filter. 1 Kohm resistor is connected for reducing the voltage level across the voltage sensor and thus it can measure the voltage. When the insulation sample is good, the voltage across the sensor after RC filter is almost 0. However, in case broken sample, the voltage across the sensor after RC filter is over than 0. This is because the capacitor is replaced with conductor and the current will flow in that branch. Based on that the magnitude of the sensed voltage is the criteria to determine the insulation sample either good or broken.

To evaluate the performance of the insulation materials of traction machine, a metal-oxide- field-effect transistor(MOSFET) to generate a semi-square wave unipolar voltage waveform with different levels of voltage power amplifier were used. The unipolar square wave voltage, which is shown in Figure 3.4 was used to implement the lifetime tests on the winding samples.

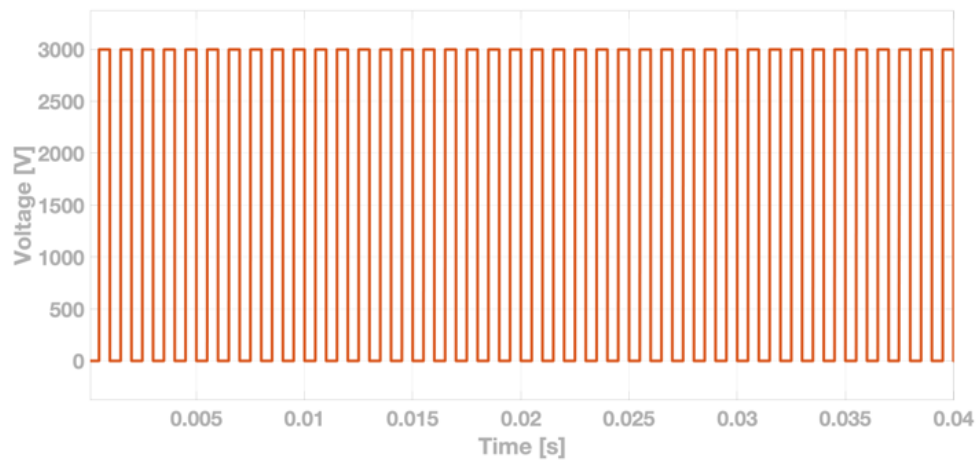


**Figure 3.4:** Applied voltage to one channel

## 3.2 The Test Procedures

The test procedure is listed in the table below. There are three different insulation materials that are tested. The test was carried on until the insulation sample was broken. The lifetime of this material is determined. Then, the sample is changed with the next material and the procedure was repeated.

Parameters	FN	ECRC 67	ECRC 53
Applied voltage (Kv)	3.5	3.5	3.5
Temperature (Degrees)	180	180	(180,150)
Frequency (Khz)	1	1	1
Duty cycle	0.5	0.5	0.5

**Table 3.1:** The insulation sample materials versus parameters

# 4

## Experiment Design

### 4.1 Winding Insulation Samples

There are three standard materials as well as three alternative materials. The six insulation materials have different specifications which are described as follow

#### 4.1.1 Kapton® FN

It is a non-resistance material has a great dielectric and thermal performance. It has a chemical resistant with being one sided laminated based adhesive.

#### 4.1.2 Kapton® FCR

It is a corona resistance material that is Featured with a laminated FEP adhesive system. This material is developed to be able to withstand the high electrical stress  $dv/dt$  from DC pulse variable frequency drives.

#### 4.1.3 Kapton® FCRC

This material has the same specifications of the previous one (FCR) but it is developed to be better for the voltage endurance. It is also laminated FEB adhesive.

#### 4.1.4 Kapton® EWS

This material is thinner than previous materials. It is used in oil and gas industry. It has a dispersion coated one-sided adhesive system.

#### 4.1.5 Kapton® ECRC

It is thin, perfect dielectric and great  $dv/dt$  resistance performance. Therefore, It is targeting the e-machine. It is coated with adhesive system from one side. It is functionalized for  $dv/dt$  resistance performance.

#### 4.1.6 Kapton® PRN

It is also used in oil and gas industry. It is coated with adhesive system from two sided with highest thermal performance. This material is characterised with perfect

chemical resistant and scrape abrasion.

The insulation lifetime test will be focused on two different materials Kapton® FN and Kapton® ECRC. The study will show the effect of both materials on the winding insulation lifetime under different experimental conditions. The insulation material sample is bending as shown in Figure 4.1 .

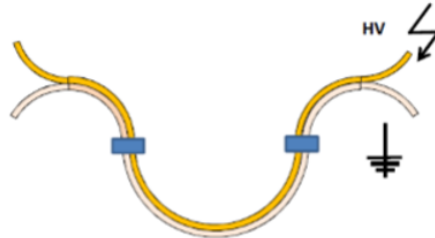


**Figure 4.1:** Test sample of insulation material

It consists of two parallel insulated wires that need to be prepared in the same way as in machine coils. One side of the sample is connected to high voltage and the other is grounded.

## 4.2 Experimental Set-ups

The electrical circuit that is illustrated in Figure 3.3, is the simulated circuit for experiment Setups where the connection between components is illustrated in Figure 4.2 .

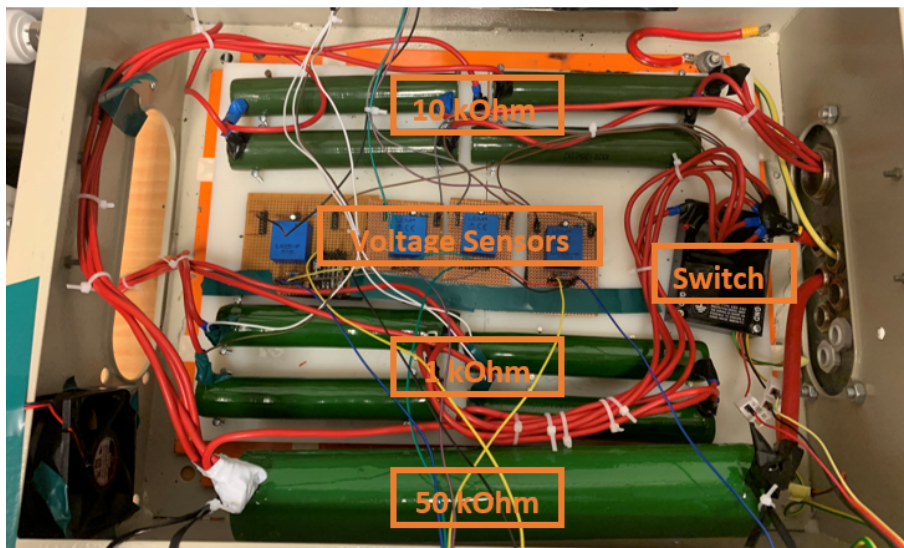


**Figure 4.2:** Test Setups

As seen in Figure 4.3 A high voltage power supply with modified voltage control is used to supply low direct current. The limit of the current is 120 (mA). The power supply is connected with a capacitance in order to stabilize the DC voltage.

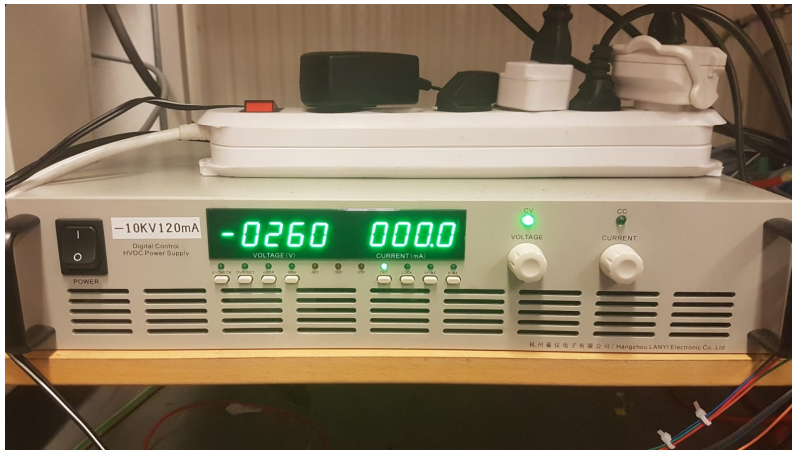


**Figure 4.3:** The high voltage power supply

The resistances ( 10, 50, 1 ) K Ohm is required in the circuit for different reasons. Besides, the switch is used for converting the DC to a square wave voltage. The switching frequency and the duty cycle is controlled by the software program that is LAB View 2019. This type of switch is a high voltage transistor. As illustrated in Figure 4.4 the switch type is BEHLKE that is designed for industrial use. The switching units can be operated between  $-40^{\circ}\text{C}$  to  $75^{\circ}\text{C}$ .



**Figure 4.4:** Fast high voltage solid state switch

The voltage sensor was used to observe the voltage across the resistor 1 Kohm. It can be used to detect the broken isolation sample. Each voltage sensor was connected with the main circuit with the low pass filter in order to eliminate the noises. The model is LEM LV25-P (717129) as seen in Figure 4.5 as follow.

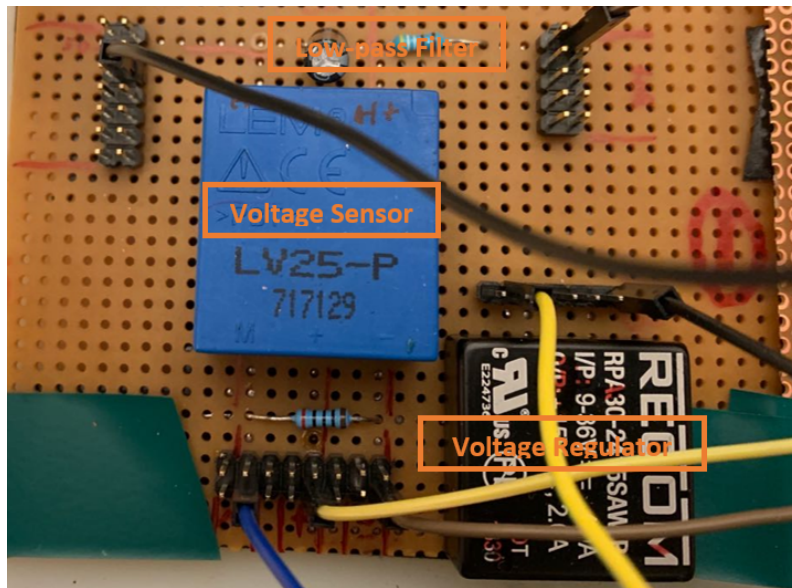


**Figure 4.5:** The voltage sensor and the low pass filter

The function of this sensor is sensing the voltage. If the voltage drop across the resistor 1 Kohm is high due to high current in case broken sample, a signal is sent to the relay to disconnect the circuit. The model of the high voltage read relay is (LRL-101-100PCV) as shown in Figure 4.6



**Figure 4.6:** high voltage read relay

Four winding samples are put in the oven to keep the environment temperature at two different temperatures (150 and 180 degrees), as can be seen in Figure 4.7 .

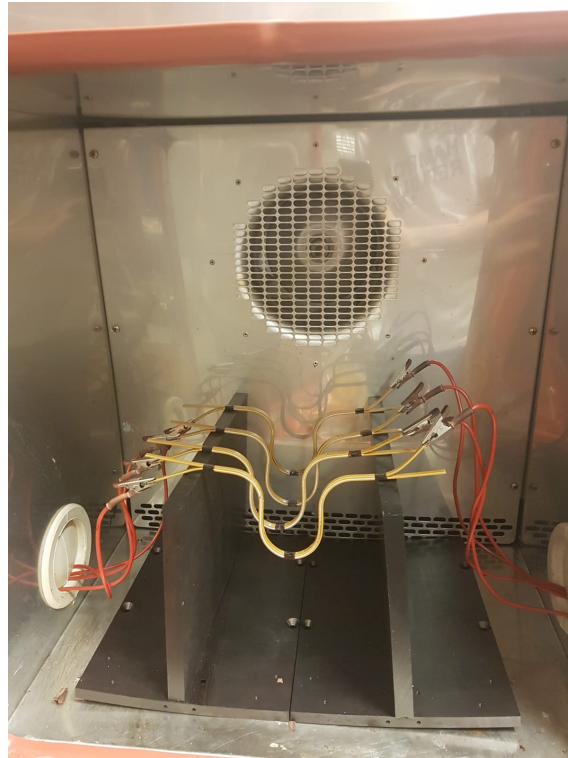


**Figure 4.7:** The four samples of insulation is put in the oven

The whole Experimental setups are monitored by two cameras in order to run the system 24 hours. The whole system is shown in Figure 4.8

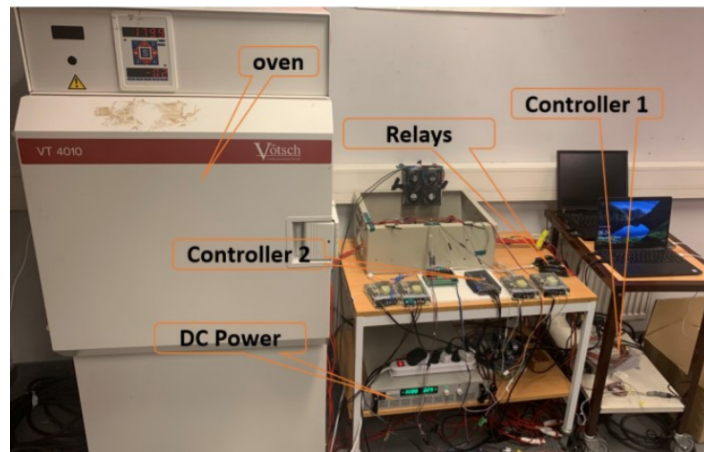


**Figure 4.8:** The whole experiment setups [22]

### 4.3 Experimental Control Strategies

There is voltage sensor for each winding sample for each branch. The voltage signal is sent to controller 1 (DSPACE) that controls also with the switch of relay for each branch. Controller 1 (DSPACE) converts signals from analog to digital and

vice versa. The MOSFET is controlled by controller 2 (BEHLKE, HTS-41). This controller sends PWM signal to MOSFET in order to be turned on or off with the frequency and duty cycle that are defined by the user. Both controllers 1 and 2 are connected with PC. The whole experimental topology is illustrated in Figure 4.10

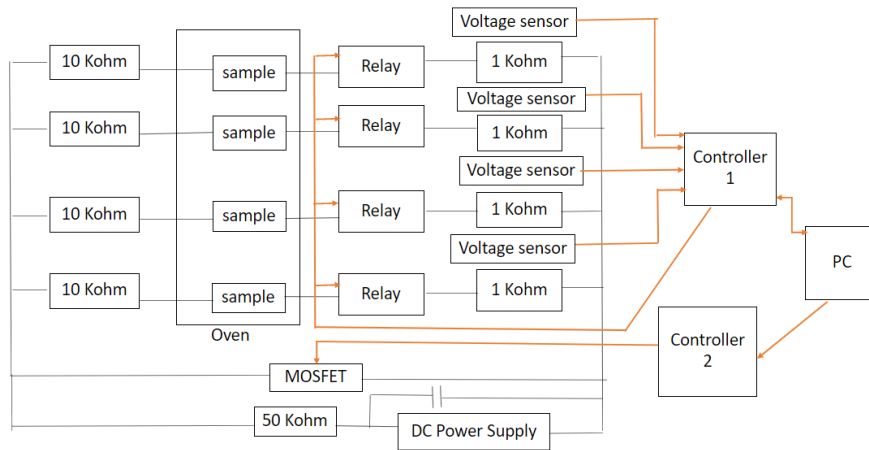


**Figure 4.9:** Experimental topology [22]

The control strategy that is taken in order to detect the insulation sample status is described in the following flowchart

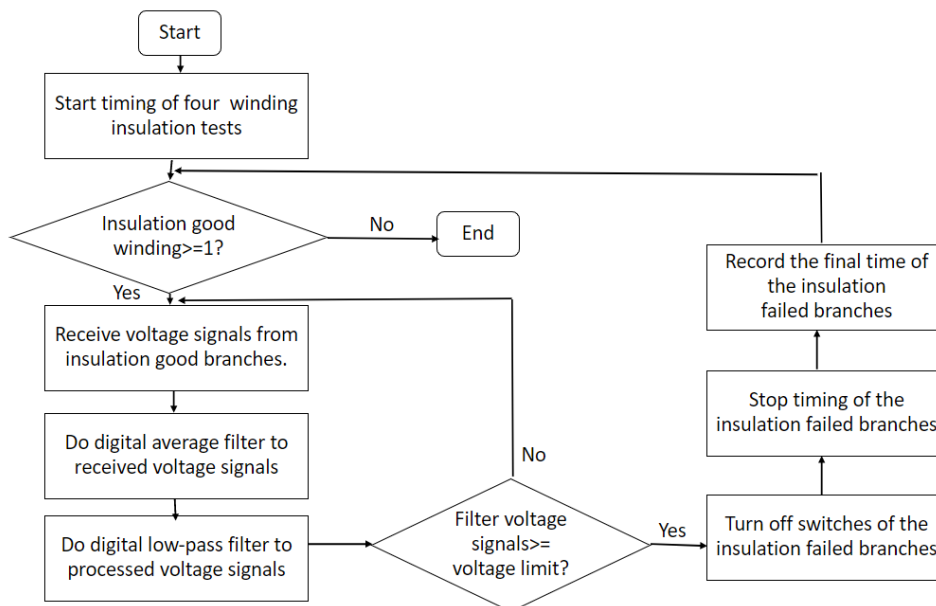


**Figure 4.10:** The flow chart of control strategy [22]

The Control Algorithms in dSPACE is illustrated in Figure 4.11. It shows that analogue digital signal (ADC) from voltage sensor pass through a digital low pass filter. If the voltage signal is lower than a specific signal, the test is continued. In this case the insulation sample is healthy. However, in case of broken sample the voltage signal becomes higher than the specific value. Then a digital analogue signal (DAC) is sent to the relay for disconnecting the circuit. The time is triggered and recorded.

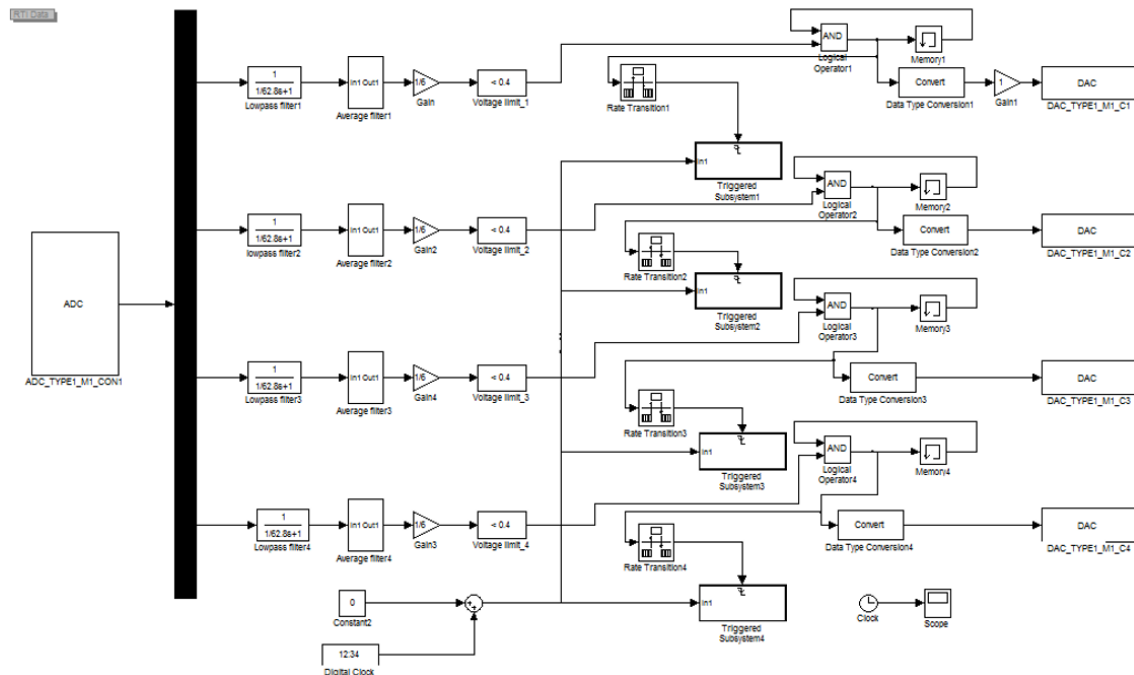


Figure 4.11: The Control Algorithms in dSPACE

# 5

## Results

### 5.1 Simulation Results

The electrical circuit is simulated by Simulink. In order to determine the winding sample insulation status whether healthy or broken sample, the next process is done as follow

In case of healthy sample, The measured voltage across 1 Kohm resistor without low pass filter is high and it is hard to measure by experiments. It is illustrated in Figure 5.1 as follow

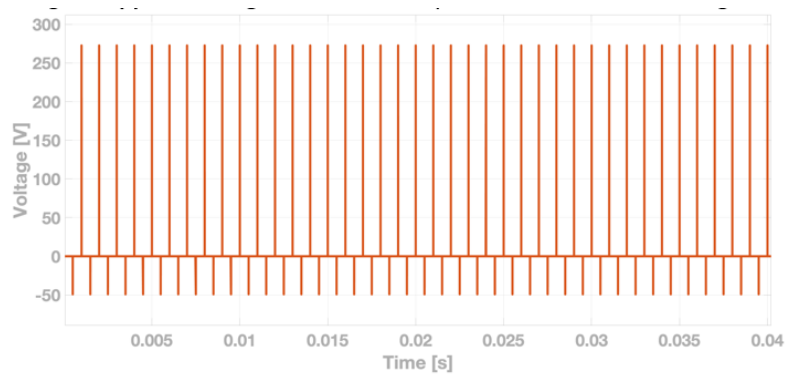


**Figure 5.1:** Measured voltage across 1 Kohm resistor, before filter (healthy sample)

In order to reduce the noise in the voltage waveform, the low pass filter is added. The voltage across 1 Kohm resistor is low in magnitude and it is almost zero as seen in Figure 5.2

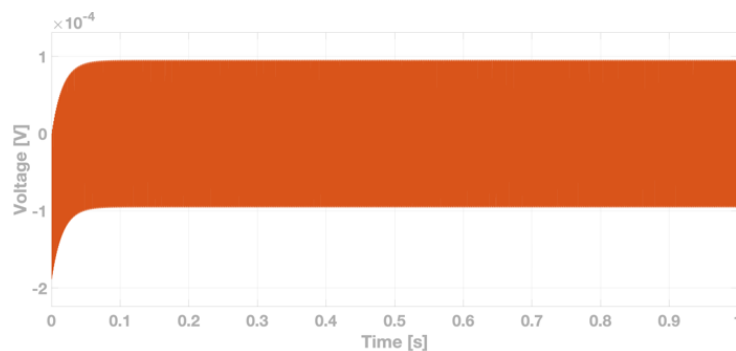


**Figure 5.2:** Measured voltage across 1 Kohm resistor, after filter (healthy sample)

In case of broken sample, The measured voltage a cross 1 Kohm resistor without

filter is also hard to measure because of the fluctuation. It is between high and zero voltage as illustrated in Figure 5.3

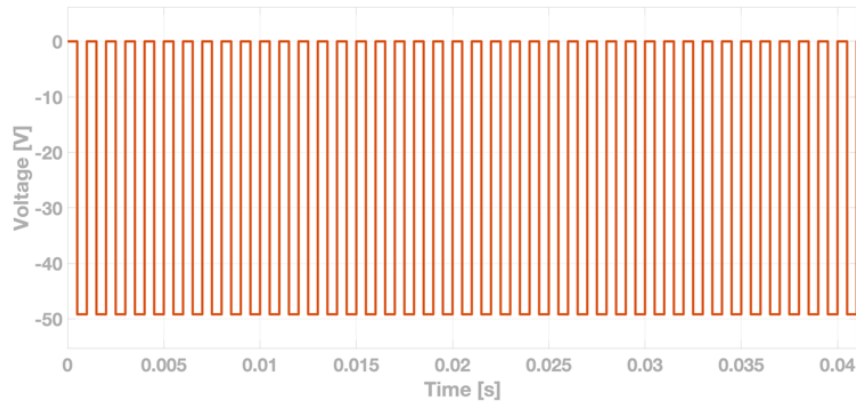


**Figure 5.3:** Measured voltage across 1 Kohm resistor, before filter (broken sample)

The measured voltage across 1 Kohm resistor with filter is more stabilized and it is easy to observed by experimental. it is shown in Figure 5.4 as follow

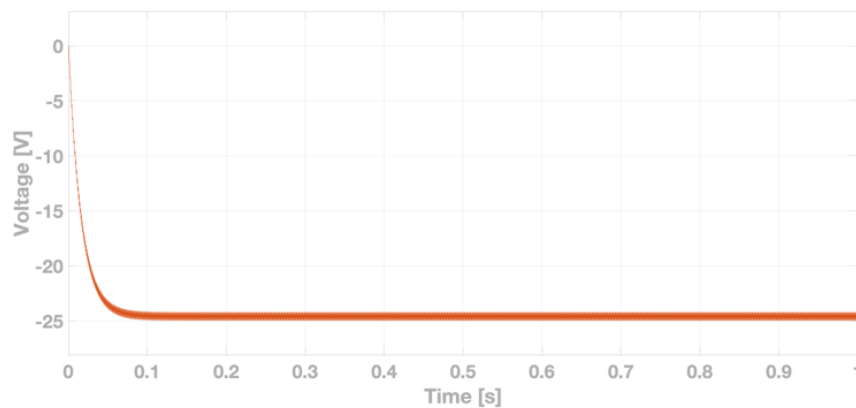


**Figure 5.4:** Measured voltage across 1 Kohm resistor, after filter (broken sample)

It is observed in case of broken sample the voltage is 25 V after filter. It is around half voltage magnitude compared with the measured voltage without filter that is around 50V.

## 5.2 Experimental Results

### 5.2.1 FN At 180 Degrees And 3.5 Kv

The first sample, which is FN, was tested at voltage 3.5 Kv and temperature 180. The results are recorded as follow:

NO	Time to insulation broken
1	5 hours
2	8 hours
3	8 hours
4	9 hours

**Table 5.1:** FN at 180 degrees and 3.5Kv

The average lifetime of FN material is calculated as:

$$LifeTime = (5.5 + 8 + 8 + 8.7)/4 = 7.55hours. \quad (5.1)$$

### 5.2.2 ECRC67 At 180 Degrees And 3.5 kV

The second important material is ECRC67. The test was done at voltage 3.5Kv and temperature 180 degree. The results are recorded as follow:

NO	Time to insulation broken
1	131.266 hours
2	156.316 hours
3	154 hours
4	121.4 hours

**Table 5.2:** ECRC67 At 180 Degrees And 3.5Kv

The average lifetime of ECRC67 material is calculated as:

$$LifeTime = (131.266 + 156.316 + 154 + 121.4)/4 = 140.75hours. \quad (5.2)$$

### 5.2.3 ECRC53 At 180 Degrees And 3.5 Kv

Now the material, which was tested, is the same previous one but the percentage is different ECRC53. The voltage and temperature are 3.5Kv, 180 respectively. The results are shown in the table below.

NO	Time to insulation broken
1	51 hours
2	60 hours
3	74 hours
4	55 hours

**Table 5.3:** ECRC53 at 180 degrees and 3.5Kv

The average lifetime of ECRC53 material is calculated as:

$$LifeTime = (51 + 60 + 74 + 55)/4 = 60hours. \quad (5.3)$$

### 5.2.4 ECRC53 At 150 Degrees And 3.5 Kv

Now the material is ECRC53 but the temperature is lower than previous one. The temperature is  $T_{em} = 150$ , and the voltage is  $V = 3.5Kv$ . The results are recorded in the table below:

NO	Time to insulation broken
1	71 hours
2	50 hours
3	92 hours
4	45.6 hours

**Table 5.4:** ECRC53 at 150 degrees and 3.5kV

The average lifetime of ECRC53 material at  $T_{em} = 150$  is calculated as:

$$LifeTime = (71 + 50 + 92 + 45.6)/4 = 64.65hours. \quad (5.4)$$

The sample, which is shown in Figure 5.5, is ECRC using 68 overlap (supported with several layers). The white powder, which appears on the film surface, is degraded organic material. The powder is an indicator that material was exposed to corona and that more exposure would generate more powder. This powder was appeared after 50 hours testing.



**Figure 5.5:** The white powder is included in the ECRC67 sample

The most influential areas of insulation materials that are affected by partial discharge are holes and air bubbles. Partial discharge occurs easily in the air bubbles compared to the dielectric material. This is because that air permittivity is less than dielectric material. If the applied voltage is higher than the partial discharge inception voltage, electric current flows in the air bubbles. The dielectric strength of insulation materials become less until breakdown. The figure 5.6 shows the broken sample where the black hole is located on the surface.



**Figure 5.6:** The failure of ECRC67 sample

# 6

## Discussion

Weibull analysis is a method that is used to determine the reliability of the insulation [11]. Depending on the lifetime data that is measured and taken in hours and the probability of failure in percentage, the Weibull distribution is formed.

The data is plotted and fitted to be a straight line. The slope of the line indicates to type and reliability of the material.

As seen in Figure 6.1 the probability of failure is 85 percent if FN material has tested for 9 hours.

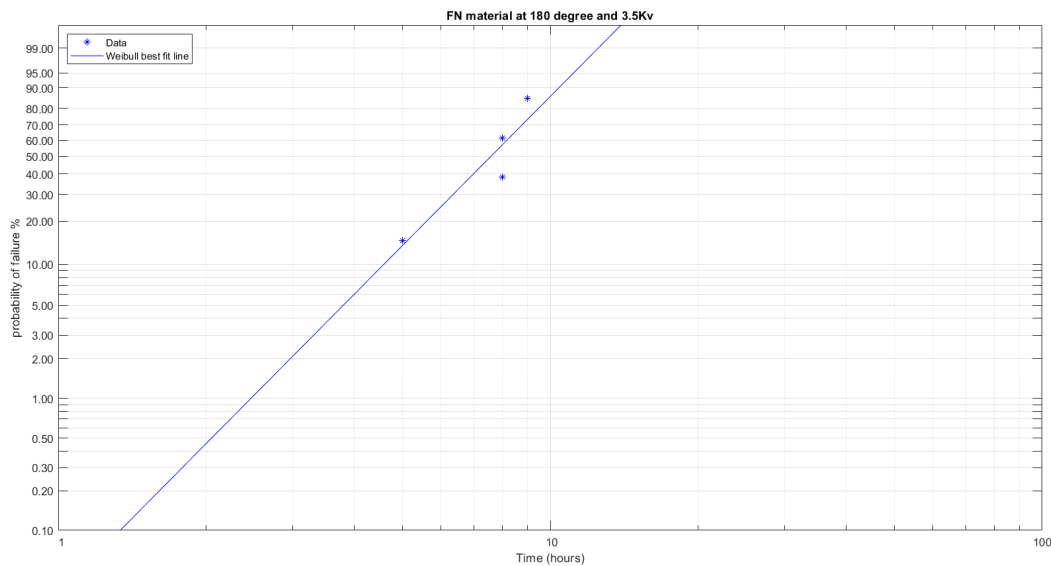


**Figure 6.1:** FN material at 180 degree and 3.5Kv

The probability of failure is 85 percent if ECRC53 overlap has tested for 74 hours as shown in Figure 6.2

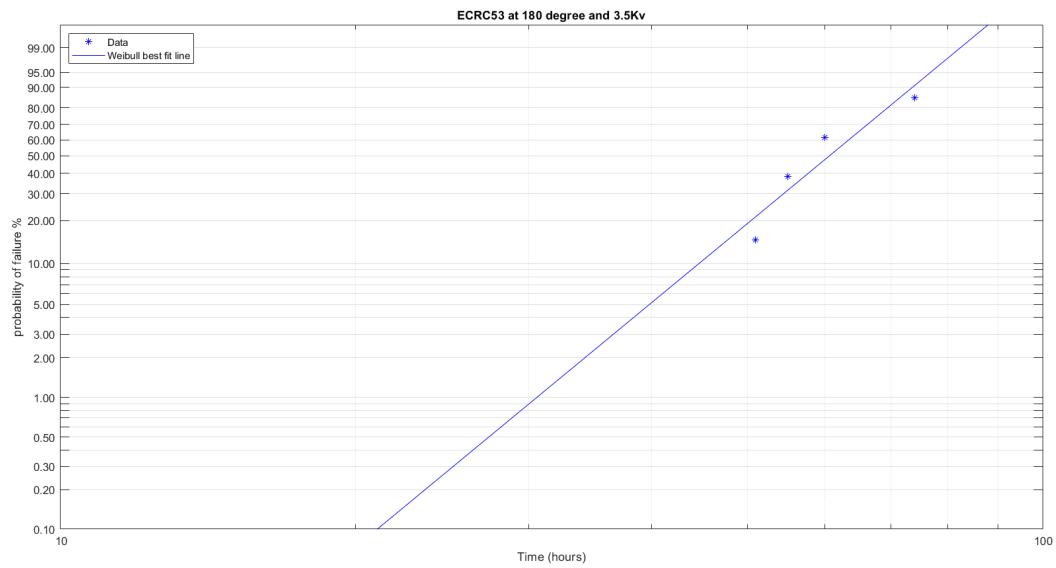


**Figure 6.2:** ECRC53 material at 180 degree and 3.5Kv

The probability of failure is 85 percent if ECRC67 overlap has tested for 157 hours as shown in Figure 6.3

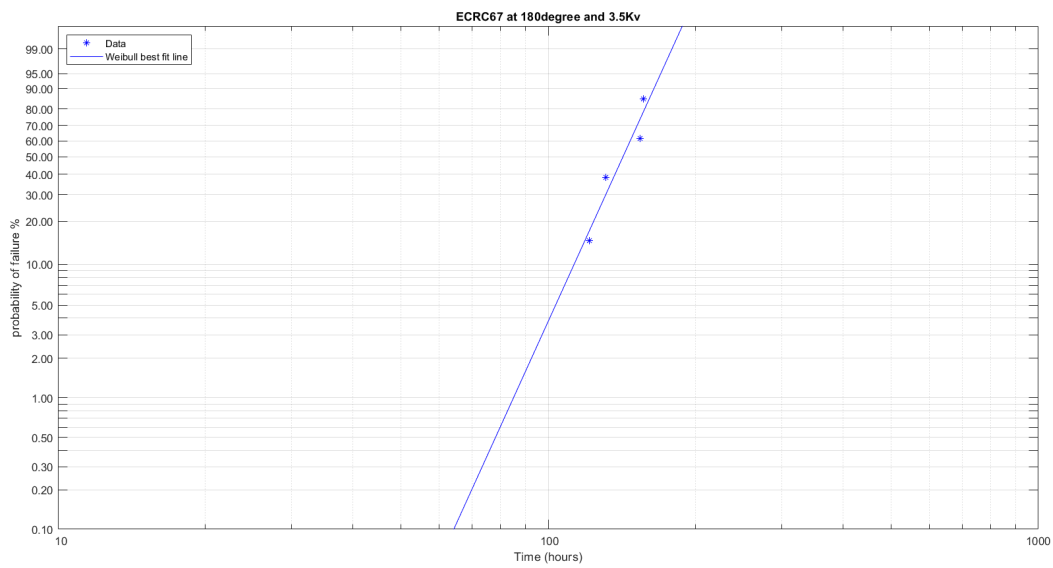


**Figure 6.3:** ECRC67 material at 180 degree and 3.5Kv

The probability of failure is 85 percent if ECRC53 overlap has tested for 95 hours as seen in Figure 6.4.

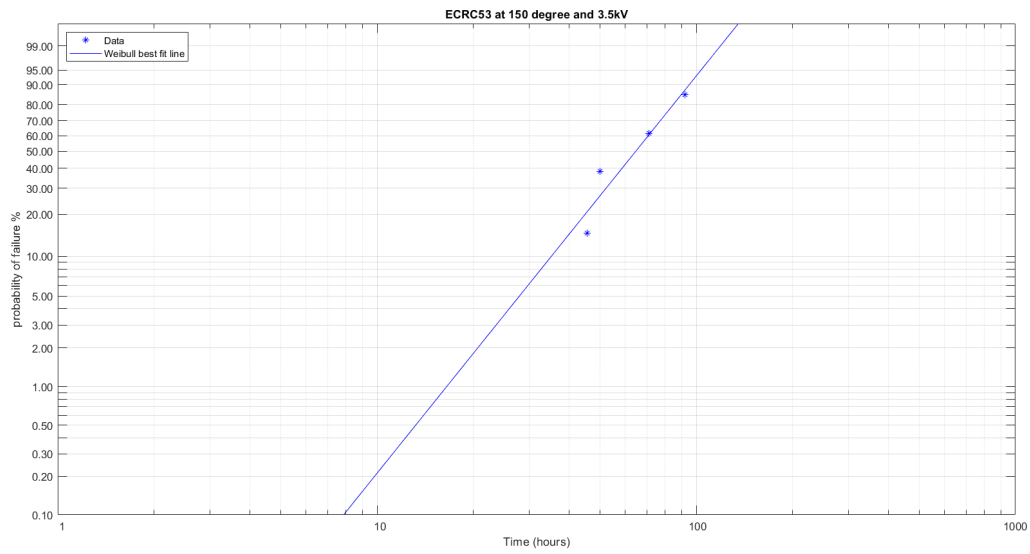


**Figure 6.4:** ECRC53 material at 150 degree and 3.5Kv

# 7

## Conclusions

The lifetime of the electric machines that are exposed to high switching frequency due to converter is extended by using advanced insulation materials. It could be using corona resistance instead of using non-corona resistance insulation materials. The results show that Corona resistance insulation materials such as ECRC increases the insulation lifetime compared with FN material(non-corona resistance material) by about 8 times. The results show as well that increasing the thickness of the material using overlap percentage will lead to increasing the insulation lifetime by about 2.3 times.

The temperature has an influence on the lifetime of the material. ECRC53 has been tested at two different levels of temperature (180,150) degrees. The difference will influence the lifetime by 7.2 times.

The test results recommend the application of corona resistant materials for conductor insulation when high switching converters are used. The thickness/overlap of the conductor insulation is a design parameter that should be decided in the design phase base on the expected thermal, electrical and mechanical stresses on the insulation system.

Future work will be focused on lower-cost production that is an important factor in the e-mobility market. Therefore, there are efforts to do more tests on enamelled corona resistance materials and compare them with standard insulation materials.

# Bibliography

1. P. Wang, A. Cavallini and G. C. Montanari, "The influence of impulsive voltage frequency on PD features in turn insulation of inverter-fed motors," 2014 IEEE Conference on Electrical Insulation and Dielectric Phenomena (CEIDP), Des Moines, IA, 2014, pp. 3538.
2. <https://www.rohm.com/news-detail?news-title=rohm-supplies-full-sic-power-modules-to-formula-e-racing-team-venturidefaultGroupId=false>.
3. <https://new.abb.com/grid/stronger-smarter-greener/powering-sustainable-transportation>.
4. P. Wang, A. Cavallini and G. C. Montanari, "The effect of impulsive voltage rise time on insulation endurance of inverter-fed motors," 2015 IEEE 11th International Conference on the Properties and Applications of Dielectric Materials (ICPADM), Sydney, NSW, 2015, pp. 8487.
5. J. Fabre, P. Ladoux, E. Solano, G. Gateau, and J. Blaqui ere, "Mvdc three-wire supply systems for electric railways: Design and test of a full sic multilevel chopper," IEEE Transactions on Industry Applications, vol. 53, no. 6, pp. 5820–5830, Nov 2017.
6. A. Rujas, V. M. L opez, A. Garc a-Bediaga, A. Berasategi, and T. Nieva, "Influence of sic technology in a railway traction dc-dc converter design evolution," in 2017 IEEE Energy Conversion Congress and Exposition (ECCE), Oct 2017, pp. 931–938.
7. A. M arz, R. Horff, M. Helsper, and M. Bakran, "Requirements to change from igbt to full sic modules in an on-board railway power supply," in 2015 17th European Conference on Power Electronics and Applications (EPE'15 ECCE-Europe), Sep. 2015, pp. 1–10.
8. M. Brenna, F. Foadelli, D. Zaninelli, and D. Barlini, "Application prospective of silicon carbide (sic) in railway vehicles," in 2014 AEIT Annual Conference - From Research to Industry: The Need for a More Effective Technology Transfer (AEIT), Sep. 2014, pp. 1–6.

9. J. Casarin, P. Ladoux, B. Chauchat, D. Dedecius, and E. Laugt, "Evaluation of high voltage sic diodes in a medium frequency ac/dc converter for railway traction," in International Symposium on Power Electronics Power Electronics, Electrical Drives, Automation and Motion, June 2012, pp. 1182–1186.
10. <http://www.behlke.com/>
11. <https://quality-one.com/weibull/>
12. Nategh.S, Berardi. G,Bianchi.N, " Inter-turn Voltage in Hairpin Winding of Traction Motors Fed by High-Switching Frequency Inverter" 2020.
13. Xiangdong Xu " Partial discharge activity studied by its excess current" 2018.
14. Peng Wang, Andrea Cavallini " The Effect of Impulsive Voltage Rise Time on Insulation Endurance of Inverter-fed Motors" 21 November 2016.
15. Xiangdong Xu " Partial discharges studied by dielectric response method" 2015.
16. WEIJUN YIN " Failure Mechanism of Winding Insulations in Inverter-Fed Motors" 1997.
17. Peng Wang, Andrea Cavallini "The influence of repetitive square wave voltage parameters on PD statistical features" 2013.
18. M. Shanel\*, J.C. Duart\*, J.G. Marchetta\*, R.C. Wicks\*\*, E. Wang\*\* and S. Ren "NOVEL SLOT AND PHASE INSULATION OPTIONS FOR MACHINES FED FROM VOLTAGE CONVERTERS" 2017.
19. <https://core.ac.uk/download/pdf/38055214.pdf>
20. <https://circuitdigest.com/article/brushed-vs-brushless-motor-operation-construction-applications>
21. Shafiqh Nategh, Yujing Liu, Xiaoliang Huang, Bowen Jiang " Accelerated Destructive Experiment Design of Motor Stator Winding Insulation Systems" 2021.
22. <https://www.embitel.com/blog/embedded-blog/brushless-dc-motor-vs-pmsm-how-these-motors-and-motor-control-solutions-work>
23. J. Lin, N. Schofield, and A. Emadi, "External-rotor 6–10 switched reluctance motor for an electric bicycle," IEEE Transactions on Transportation

and Electrifications, vol. 1, no. 4, pp. 348–356, Dec. 2015.

24. K. W. Hu, Y. Y. Chen, and C. M. Liaw, “A reversible position sensorless controlled switched-reluctance motor drive with adaptive and intuitive commutation tunings,” *IEEE Transactions on Power Electronics*, vol. 30, no. 7, pp. 3781–3793, Jul. 2015.